11-7-2016

# Compartmentalized Metabolic Engineering for Artemisinin Biosynthesis and Effective Malaria Treatment by Oral Delivery of Plant Cells

Karan Malhotra

Mayavan Subramaniyan

Khushboo Rawat

Md. Kalamuddin

M. Irfan Qureshi

*See next page for additional authors*



## Recommended Citation

Malhotra, K., Subramaniyan, M., Rawat, K., Kalamuddin, M., Qureshi, M. I., Malhotra, P., Mohmmed, A., Cornish, K., Daniell, H., & Kumar, S. (2016). Compartmentalized Metabolic Engineering for Artemisinin Biosynthesis and Effective Malaria Treatment by Oral Delivery of Plant Cells. *Molecular Therapy, 9* (11), 1464-1477. http://dx.doi.org/10.1016/j.molp.2016.09.013

# Compartmentalized Metabolic Engineering for Artemisinin Biosynthesis and Effective Malaria Treatment by Oral Delivery of Plant Cells


## Abstract

Artemisinin is highly effective against drug-resistant malarial parasites, which affects nearly half of the global population and kills >500 000 people each year. The primary cost of artemisinin is the very expensive process used to extract and purify the drug from *Artemisia annua*. Elimination of this apparently unnecessary step will make this potent antimalarial drug affordable to the global population living in endemic regions. Here we reported the oral delivery of a non-protein drug artemisinin biosynthesized (~0.8 mg/g dry weight) at clinically meaningful levels in tobacco by engineering two metabolic pathways targeted to three different cellular compartments (chloroplast, nucleus, and mitochondria). The doubly transgenic lines showed a three-fold enhancement of isopentenyl pyrophosphate, and targeting AACPR, DBR2, and CYP71AV1 to chloroplasts resulted in higher expression and an efficient photo-oxidation of dihydroartemisinic acid to artemisinin. Partially purified extracts from the leaves of transgenic tobacco plants inhibited *in vitro* growth progression of *Plasmodium falciparum*-infected red blood cells. Oral feeding of whole intact plant cells bioencapsulating the artemisinin reduced the parasitemia levels in challenged mice in comparison with commercial drug. Such novel synergistic approaches should facilitate low-cost production and delivery of artemisinin and other drugs through metabolic engineering of edible plants.



## Keywords

bioencapsulation, oral delivery of plant material, dihydroartemisinic acid, isopentenyl pyrophosphate, plant transformation, drug biosynthesis


## Disciplines

Dentistry


## Author(s)

Karan Malhotra, Mayavan Subramaniyan, Khushboo Rawat, Md. Kalamuddin, M. Irfan Qureshi, Pawan Malhotra, Asif Mohmmed, Katrina Cornish, Henry Daniell, and Shashi Kumar

HHS Public Access

Author manuscript

*Mol Plant*. Author manuscript; available in PMC 2018 May 31.

Published in final edited form as:

*Mol Plant*. 2016 November 07; 9(11): 1464–1477. doi:10.1016/j.molp.2016.09.013.

# Compartmentalized Metabolic Engineering for Artemisinin Biosynthesis and Effective Malaria Treatment by Oral Delivery of Plant Cells

**Karan Malhotra**[1], **Mayavan Subramaniyan**[1], **Khushboo Rawat**[2], **Md. Kalamuddin**[2], **M. Irfan Qureshi**[3], **Pawan Malhotra**[2], **Asif Mohmmed**[2], **Katrina Cornish**[4], **Henry Daniell**[5], and **Shashi Kumar**[1,*]

[1]Metabolic Engineering Group

[2]Malaria Research Group International Centre for Genetic Engineering and Biotechnology, Aruna Asaf Ali Marg, New Delhi 110067, India

[3]Department of Biotechnology, Jamia Millia Islamia, New Delhi 110025, India

[4]Department of Horticulture and Crop Science, The Ohio State University, Wooster, OH 44691, USA

[5]Department of Biochemistry, School of Dental Medicine, University of Pennsylvania, Philadelphia, PA 19104, USA

## Abstract

Artemisinin is highly effective against drug-resistant malarial parasites, which affects nearly half of the global population and kills >500 000 people each year. The primary cost of artemisinin is the very expensive process used to extract and purify the drug from *Artemisia annua*. Elimination of this apparently unnecessary step will make this potent antimalarial drug affordable to the global population living in endemic regions. Here we reported the oral delivery of a non-protein drug artemisinin biosynthesized (~0.8 mg/g dry weight) at clinically meaningful levels in tobacco by engineering two metabolic pathways targeted to three different cellular compartments (chloroplast, nucleus, and mitochondria). The doubly transgenic lines showed a three-fold enhancement of isopentenyl pyrophosphate, and targeting AACPR, DBR2, and CYP71AV1 to chloroplasts resulted in higher expression and an efficient photo-oxidation of dihydroartemisinic acid to artemisinin. Partially purified extracts from the leaves of transgenic tobacco plants inhibited *in vitro* growth progression of *Plasmodium falciparum*-infected red blood cells. Oral feeding of whole intact plant cells bioencapsulating the artemisinin reduced the parasitemia levels in challenged mice in comparison with commercial drug. Such novel synergistic approaches should facilitate low-cost

*Correspondence: Shashi Kumar (skrhode@icgeb.res.in).

**SUPPLEMENTAL INFORMATION**

Supplemental Information is available at *Molecular Plant Online*.

**AUTHOR CONTRIBUTIONS**

K.M. performed experimental analysis on double transgenics generated by M.S. K.M., K.R., and M.K. conducted *in vitro* and animal studies under the supervision of P.M. and A.M. M.I.Q. and K.C. coordinated the studies. S.K. and H.D. conceived the concept. S.K. designed and facilitated the study. K.M. and S.K. wrote and edited the manuscript with the help of P.M., A.M., K.C., and H.D.

production and delivery of artemisinin and other drugs through metabolic engineering of edible plants.

**Keywords**

bioencapsulation; oral delivery of plant material; dihydroartemisinic acid; isopentenyl pyrophosphate; plant transformation; drug biosynthesis

## INTRODUCTION

Artemisinin-based combination therapies, commonly referred to as ACTs, are the frontline treatments in the fight against malaria (Dalrymple, 2013). Besides the antiplasmodial activity of artemisinin and its semi-synthetic derivative artesunate, the drug has demonstrated cytotoxicity against cancer cells and schistosomiasis (Efferth, 2006; Utzinger et al., 2007; Efferth et al., 2011). A notable broad-spectrum activity of artesunate has been reported against human cytomegalovirus, which has become resistant to traditional drugs such as ganciclovir (Shapira et al., 2008). However, these therapies are not readily available to patients in endemic regions due to the low yield of artemisinin from the native plant. Artemisinin is biosynthesized mainly in the glandular trichomes on leaves. Three key enzymes of artemisinin biosynthesis were exclusively expressed in apical cells of glandular trichomes but not in the subapical chloroplast-containing cells, although all of these cells did express the farnesyl pyrophosphate synthase (Olsson et al., 2009). Artemisinin production in aerial parts of the plant is sensitive to variation in genetic backgrounds, cultivation conditions, and harvesting periods. Its biosynthesis is stimulated by biotic and abiotic stress (Ferreira et al., 1995; Davies et al., 2009, 2011). The yield of artemisinin (~0.5% on dry weight basis) from *Artemisia annua* is relatively low when cultivated under Indian climatic conditions (Brisibe and Chukwurah, 2014), which limits its commercial production and value. Even the high-yield variety “CIM-Arogya,” developed for marker-assisted breeding, has maximum reported yields of ~1% in Indian conditions (Khanuja et al., 2008). Endeavors to increase artemisinin levels in *A. annua* by elicitor or hormone treatments (Smith et al., 1997; Baldi and Dixit, 2008) have met with limited success, and present efforts rely mostly on marker-assisted breeding of high-yield varieties (Graham et al., 2010). Low yields of artemisinin from crop-based production systems and the high cost of chemical synthesis, make these approaches impractical for commercial production (Enserink, 2005; White, 2008). Further to these issues, yearly variations in the availability of starting raw materials and unpredictable demand for this antimalarial agent greatly affect the price of artemisinin (Kindermans et al., 2007). Thus, alternative heterologous production platforms should be explored to address these issues. Attempts have been made to produce its precursor, amorphadiene, via metabolic engineering of *Escherichia coli* with the mevalonate (MEV) pathway and the amorphadiene synthase gene (*ADS*). Unfortunately, transgene expression inhibited *E. coli* growth, resulting in very low amorphadiene levels (Martin et al., 2003). The semi-synthetic approach in yeast yielded a high level of artemisinic acid, a precursor of artemisinin (Paddon et al., 2013), but complete biosynthesis of artemisinin was not accomplished. Expression of artemisinin is difficult in microbial hosts, mainly due to lack of plant cytochrome P450. The successive oxidation of amorphadiene to artemisinic alcohol is

catalyzed by a cytochrome P450 oxidase gene (CYP71AV1). Artemisinin biosynthesis is favored through the dihydroartemisinic acid (DHAA) biosynthetic pathway using double bond reductase 2 (DBR2), which reduces the Δ11(13) double bond of artemisinic aldehyde (Covello, 2008; Zhang et al., 2008). The conversion of DHAA to artemisinin is a non-enzymatic photochemical oxidation process (Brown and Sy, 2004).

Tobacco became our platform of choice because artemisinin is a plant product and other terpenoids have successfully been expressed (Ikram et al., 2015). Tobacco is a large plant that can be harvested several times a year and can be grown as a perennial. Each plant produces nearly a million seeds per season, so production acreage can be rapidly scaled up for the low costs production of pharmaceuticals (Arlen et al., 2007). The constitutive expression of the *ADS* gene in *Nicotiana tabacum* has been achieved (Wallaart et al., 2001) but very low levels of amorphadiene biosynthesis were realized (<2 ng/g of fresh weight). Recently, the complete biosynthesis of artemisinin was reported in *N. tabacum* via nuclear transformation by expressing *CYP71AV1* and cytochrome P450 reductase (*CPR*), along with *ADS*, *DBR2*, and a deregulated form of *HMGR* (Farhi et al., 2011a). However, artemisinin levels were found to be low in these transgenic lines (6.8 μg/g dry weight), which may be attributed to a limiting pool of isopentenyl pyrophosphate (IPP).

Subcellular targeting of ADS to mitochondria significantly improved the accumulation of amorphadiene (Wu et al., 2006; van Herpen et al., 2010; Farhi et al., 2011b). These studies showed that farnesyl pyrophosphate (FPP) (a precursor to amorphadiene) is readily available in different cellular compartments and could be utilized for amorphadiene and artemisinin biosynthesis. Chloroplasts offer an ideal platform for accumulating large amounts of IPP and overcome substrate limitations apparent in the cytosol. Homoplastomic plants engineered with the MEV pathway accumulate higher levels of mevalonate than untransformed plants (Kumar et al., 2012). Previously, we attempted to achieve complete artemisinic acid biosynthesis in tobacco chloroplasts by introducing both MEV and artemisinic acid pathways (~12 genes). Unfortunately, this approach resulted in a low yield of artemisinic acid and stunted the growth of transgenic plants (Saxena et al., 2014), possibly because of suppression of one of the added pathways or precursor limitations.

To overcome these limitations, we developed a novel strategy for complete artemisinin biosynthesis in tobacco through combining expression in both chloroplast and nuclear genomes (Figure 1). The stable doubly transgenic (DT) plants produced adequate levels of artemisinin, and drug functionality was studied on the malarial parasite *Plasmodium* using *in vitro* and *in vivo* assays.

## RESULTS

### Confirmation of Plant Transformation and Molecular Analysis

Homoplastomic plants expressing the mevalonate pathway grew similarly to wild-type plants in the greenhouse, without observable phenotypic abnormality (Supplemental Figure 1C). The functionality of the yeast mevalonate biosynthetic pathway in T-MEV plants was confirmed by treatment of transplastomic plants with selection medium containing 100 μM fosmidomycin, a specific inhibitor of 1-deoxy-D-xylulose 5-phosphate reductoisomerase

(DXR). These transplastomic plants thrived (Supplemental Figure 1D, right), while the wild-type plants had stunted growth and bleached leaves (Supplemental Figure 1D, left), confirming that IPP was produced in chloroplast by the genetically engineered mevalonate pathway (Supplemental Figure 1D, right).

Twelve independent nuclear transgenic lines were regenerated on double-selection media when T-MEV was re-transformed via *Agrobacterium tumefaciens* (strain EHA105) harboring a binary vector pNuc-Cox-Art containing DHAA biosynthetic pathway genes (Figure 2A). PCR analysis using ADS and DBR2 gene-specific primers confirmed the integration of transgenes into the nuclear genome in all 12 DT plants. All transgenic lines showed 539-bp and 441-bp amplicons for ADS and DBR2, respectively (Figure 2B). No PCR amplification product was observed in wild-type plants. All DT plants grew normally and set flowers and fertile seeds (Figure 2C). No morphological abnormality was observed in DT plants with respect to growth pattern, leaf size, or plant height when compared with wild-type plants. However, there was a decrease in the total chlorophyll and carotenoid content in all DT lines (DT1–DT4), with DT2 and DT4 showing the lowest pigment levels (Supplemental Figure 6A). Pigment levels were unaffected in the T-MEV plants. Maximum quantum yield ($F_v/F_m$), i.e., photosynthetic performance, was marginally lower in all DT lines (except DT3 and T-MEV) (Supplemental Figure 6B). The effective quantum yield, or Y(II) and Y(NPQ), or quantum yield of regulated energy dissipation, was lower for DT3 and T-MEV plants (Supplemental Figure 6C) than for the other DT plants or the wild type. As predicted, only T1 seeds from DT plants were able to grow on double-selection RMOP medium containing hygromycin (50 mg/l) and spectinomycin (500 mg/l) (Figure 2D).

The highest yield of artemisinin was observed in four lines, named DT1 to DT4, ranging from 0.3 to 0.8 mg/g dry weight. All four lines (DT1–DT4) contained a single integrated copy of the DHAA biosynthetic transgene cassette (Figure 2E). Amplicon signals of 219 bp for ADS, 281 bp for *DBR2*, 190 bp for *CYP71AV1*, and 275 bp for AACPR were observed in greenhouse-grown DT1–DT4 plants (Figure 2F), confirming nuclear expression.

## Production of Artemisinin, DHAA, IPP/Dimethylallyl Pyrophosphate, and Amorphadiene in Transformed Plants

All doubly transgenic (DT) lines accumulated artemisinin except DT9 and DT10 (Supplemental Table 3). Maximum biosynthesis was observed in DT1, DT2, DT3, and DT4. These lines accumulated artemisinin due to the non-enzymatic reaction of photo-oxidation of DHAA (Figure 3B), while no such accumulation was observed in wild-type tobacco plants (Figure 3A). The levels of artemisinin in the four transgenic lines varied between 0.3 and 0.8 mg/g dry weight (n = 3). The artemisinin content was highest in DT4 (Figure 3B and 3C) plants, about 0.8 mg/g dry weight (n = 3). The product ion (MS2) spectra of artemisinin in DT4 plant is mentioned in Supplemental Figure 2B. Such variation in transgene expression among nuclear transgenic lines is expected and occurs due to positional effects, gene silencing, and other regulatory controls.

We analyzed the synthesis of two intermediates of the artemisinin biosynthetic pathway, namely DHAA and IPP, in the transgenic lines DT1–DT4. A peak corresponding to the retention time of DHAA was observed in both a DHAA standard (Figure 4A) and an extract

of *A. annua* (Figure 4C). Interestingly, an additional peak at 5.2 min was observed in the DTs (Figure 4B), which matched the chromatographic profile of *A. annua* (Figure 4C) used as a control. However, this additional peak was not observed in the authentic standard of DHAA (Figure 4A). Maximum DHAA accumulation observed was in DT4, up to 150 μg/g dry weight (Figure 4B).

Intermediate metabolite IPP synthesis in the DTs was compared with the wild-type plants, using an authentic standard of IPP (Supplemental Figure 3B) by liquid chromatography–tandem mass spectrometry (LC–MS/MS). The DT plants accumulated more IPP (Figure 5C–5E) than the wild type (Figure 5A) and T-MEV plants (Figure 5B). The mean amount of IPP ranged from 0.1 to 2.5 μg/g fresh weight in DTs, compared with only ~0.07 μg/g fresh weight in the wild type (n = 3, Figure 5G). The intermediate volatile metabolite amorphadiene was detected in DTs by gas chromatography (GC)–MS by comparing the mass spectra with the standard (Figure 6A and 6B). The transgenic line DT4 (Figure 6A, upper chromatogram) had the highest amorphadiene levels, up to 60 μg/g dry weight. However, absolute quantification of this compound is difficult due to the volatile nature of amorphadiene (Beale et al., 2006; van Herpen et al., 2010).

### *In Vitro* Anti-parasitic Activity of Artemisinin Produced by DTs

Partially purified transgenic plant extracts of DT lines inhibited the growth of parasites after 24 and 48 h (Figure 7A). Few or no new ring-stage parasites, and dead parasites with constricted and shrunken morphology, were observed (Figure 7A). In comparison, parasite cultures treated with either DMSO or with an extract from wild-type plants grew normally. The merozoites released from schizonts further invaded fresh red blood cells (RBCs) and formed new rings by 48 h (Figure 7A). Extract from DT4, which contained the highest artemisinin level, was most effective, with $IC_{50}$ ~79 nM (Figure 7B; see also Supplemental Figure 4).

### Efficacy of Artemisinin-Producing Plant Extracts in the *P. berghei* Mouse Model

The *in vivo* anti-malarial efficacy of DT plant extracts was analyzed using the *Plasmodium berghei* murine malaria model. Infected mice were fed with dried intact plant cells using a gavage needle, and parasitemia was evaluated every day until day 15. Parasitemia profiles of mice treated with transgenic plants were compared with mice fed with pure artemisinin drug or wild-type plant extracts. Similar progression in parasitemia was observed in mice fed with pure artemisinin as well as those fed with the wild-type plant extract (Figure 7C), the control group. However, mice fed with crushed DT leaves showed a considerable delay in progression of parasitemia, most notable in mice fed with DT4 on the 10th day post infection. A significant reduction in parasitemia from ~2.5% to ~1.6% was observed when compared with mice fed pure artemisinin (Figure 7C). In addition, mice fed with DT4 leaf material did not show any sign of malarial sickness during the first week of infection, while mice fed with pure artemisinin or wild-type plants had malarial symptoms. Together, these results show that DT leaf material considerably delayed the development of parasitemia in mice and that this delay was longer than that induced by pure artemisinin.

## DISCUSSION

In our previous study (Saxena et al., 2014), expression of all the 12 transgenes into the tobacco chloroplast genome caused stunted growth, which highlighted the need to spread the biosynthetic load to more than one metabolic compartment. We circumvented these defects by using a balanced compartmentalization approach to transgene expression using three cellular compartments (cytosol, chloroplast, and mitochondria), and obtained DT plants with normal phenotypes and up to 0.8 mg artemisinin per gram dry weight leaf. A similar effort using combinatorial super transformation of transplastomic lines engineered with the artemisinic acid pathway resulted in an accumulation of 120 μg/g fresh weight of artemisinic acid (Fuentes et al., 2016). Low artemisinin accumulation in tobacco in earlier reports was thought to be either due to a high level of glycosylation by endogenous glycosyl transferases (van Herpen et al., 2010; Ting et al., 2013) or unfavorable cytosolic environmental conditions preventing the formation of late-stage artemisinin precursors (Zhang et al., 2011). The transgenes *AACPR*, *CYP71AV1*, and *DBR2*, beyond *ADS*, were targeted to the chloroplast in our study because it is a glycosylation-free compartment. Thus, chloroplasts offer ideal sites for accumulation of complex transgene products that may otherwise be harmful if accumulated in the cytosol (Bogorad, 2000). The use of intense light during greenhouse cultivation and harvesting of DT lines may have favored the bioconversion of DHAA to artemisinin by photo-oxidation (Farhi et al., 2011b). Also, the excess pool of IPP/dimethylallyl pyrophosphate (DMAPP), produced in the DT plants (via T-MEV pathway and *IDI* gene expressed in chloroplast and nuclear genome, respectively) may have helped produce the higher end product. We hypothesize that compartmentalization, subcellular targeting of artemisinin biosynthetic enzymes to chloroplasts, and a surplus amount of endogenous IPP (Figure 5B) are key to producing much higher levels of artemisinin than previously reported (Supplemental Table 2).

All terpenoids, including artemisinin, are synthesized from two isoprenoid precursors, IPP and DMAPP. However, the synthesis of IPP by the MEV pathway is tightly regulated due to its need to supply diverse metabolic processes (Goldstein and Brown, 1990). The limited, wild-type, IPP pool is unlikely to permit DHAA accumulation and would result in the little biosynthesis of artemisinin. LC–MS/MS measures the total amount of IPP and DMAPP as both the metabolites are allylic isomers with the same parent mass, i.e., 245 Da (Li and Sharkey, 2013); thus, in our analysis the total amount of IPP and DMAPP was quantified (Figure 5A–5G). The IDI gene (IPP/DMAPP isomerase) was introduced into the nuclear genome, which may have helped to maintain a favorable equilibrium between IPP and DMAPP, and normal physiological functions in eukaryotes (Koyama et al., 1983; Lützow and Beyer, 1988). Moreover, reduced IDI activity affects isoprenoid biosynthesis in the plastids of tobacco leaves and results in depletion of photosynthetic pigments (Page et al., 2004). Amorphadiene is the first committed precursor in the artemisinin biosynthetic pathway. Previous reports suggest that fusion of sesquiterpene synthases with cox4 results in elevated levels of sesquiterpenoid production because of the considerable pool of FPP found in mitochondria (Kappers et al., 2005; Farhi et al., 2011b). Therefore, to enhance amorphadiene synthesis, the *ADS* gene was fused with mitochondrial signal peptide (cox4), and this did result in higher amorphadiene biosynthesis (Figure 6A).

Previously, we have reported the expression of individual transgenes related to the MEV pathway in chloroplasts (Kumar et al., 2012). The RT–PCR study was conducted for mRNA analysis for determining the expression of other essential transgenes (*DBR2*, *ADS*, *AACPR*, and *CYP71AV1*). The weak correlations between mRNA and protein expression are attributed to various post-transcriptional processes that complicate accurate estimates of quantities of the corresponding mRNAs destined for translation (Gry et al., 2009; Vogel and Marcotte, 2012). Furthermore, it may be difficult to decipher accumulation of individual metabolites in chloroplasts using the metabolomics approach, as native MEV/MEP (methylerythritol-4-phosphate) pathways also function in plants.

Studies on *A. annua* high-artemisinin-producing and low-artemisinin-producing chemotypes suggest different biosynthetic routes beyond artemisinic aldehyde intermediate (Bertea et al., 2005; Covello, 2008). The two chemotypes had different *CYP71AV1* enzyme activities (Ting et al., 2013), and the activity of the *Dbr*2 promoter also was implicated (Yang et al., 2015). We chose a strong constitutive promoter, the 35S promoter of CaMV with double enhancer, to drive the expression of *Dbr*2 gene and thereby generate excess *DBR2* transcripts, to favor artemisinic aldehyde flux toward DHAA and eventually artemisinin biosynthesis.

There were no adverse effects on the growth or morphology of DT plants producing artemisinin (Supplemental Figure 6A), and the minor decrease in pigments had no observable effect on the whole plants. Nonetheless, the pigment decrease in DT2 and DT4 may have been caused by the consumption of IPP by the artemisinin pathway. The marginally lower Y(NPQ), in DT3, most likely explains the reduced Y(II) value (Supplemental Figure 6C). In general, a high Y(NPQ) value indicates that plants are more adapted to light stress and more efficiently direct it toward photosynthesis (Gao et al., 2011).

In our case, the co-expression of two pathways did not imbalance plant metabolism to a sufficient degree to cause gross aberrant effects. This is in contrast to a recent report, which found extensive off-target effects induced by overexpression, in tobacco, of FPP synthase and squalene synthase in the cytosol, chloroplast, or both. Their large changes were attributed to metabolite-mediated anterograde and/or retrograde signaling regardless of the level of transgene expression or end product, due to imbalanced metabolic pools (Pasoreck et al., 2016). These negative impacts were not related to the number of genes expressed or the level of expression. However, it is possible that our co-expression strategy to increase the pool IPP and the physiological regulator IDI provided the observed metabolic balance not observed by Pasoreck et al. (2016). IPP does appear to pass between the chloroplastic and cytosolic compartments independent of the synthetic site (Bick and Lange, 2003; Dudareva et al., 2005; Kumar et al., 2012). This is supported by our study on the levels of squalene in untransformed (wild-type), chloroplast transformed (T-MEV), and chloroplast and nuclear transformed (DT) plants. GC–MS/MS analysis showed a significant increase in the overall yield of squalene in DT and T-MEV plants compared with wild-type plants (Supplemental Figure 7), which could be due to a unidirectional transport of metabolites across the chloroplast envelope membrane or to direct effects of excess FPP. However, low levels of squalene were present in the high-artemisinin-producing DT2 and DT4 (Table 1), indicating a preferential consumption of IPP and FPP by the artemisinin pathway in these plants.

The primary cost of artemisinin is the very expensive process used to extract and purify the drug from *A. annua*. Our report indicates that this is an unnecessary step and that artemisinin can be produced in edible leaves. We provide a proof-of-concept demonstration of the functionality of tobacco-biosynthesized artemisinin in DT lines. This finding suggests that artemisinin can become accessible and affordable to the large global population living in malarial regions. Malaria remains a global health problem with nearly 3.2 billion people at risk (almost half of the world's population) (http://www.who.int/mediacentre/factsheets/fs094/en/). Results demonstrated through *in vitro* (Figure 7A) and *in vivo* animal studies (Figure 7A and 7B) are critical for functional evaluation of foreign products expressed in plants.

Earlier reports had shown that none of the substances in tobacco leaves, including nicotine, reduced the parasitemia load when wild-type tobacco leaves were fed orally to mice (Davoodi-Semiromi et al., 2010). Mice fed orally with extracts from wild-type and commercially available pure drug resulted in similar parasite loads. This was probably due to the poor bioavailability of the pure (commercial) artemisinin, which is rapidly degraded by hepatic and intestinal cytochrome enzymes (Svensson and Ashton, 1999). The enhanced efficacy of artemisinin delivered via intact whole-plant DT4 leaves compared with pure (commercial) artemisinin is probably due to the bioencapsulation of this bioactive compound. A previous report on the oral feeding of *A. annua* (Weathers et al., 2014; Elfawal et al., 2015) suggested that higher efficacy of orally fed *A. annua* leaves could be due to the protection of flavonoids or other antioxidants present in plants or animal feed. We have previously shown that plant cells protect biopharmaceuticals from acids and enzymes in the stomach via bioencapsulation. The gut microbes release these drugs in the gut lumen by the action of commensal microbes, where they are absorbed and delivered to the blood circulation system (Limaye et al., 2006; Kwon et al., 2013; Kohli et al., 2014; Sherman et al., 2014; Shil et al., 2014). Human digestive enzymes are incapable of breaking down glycosidic bonds in plant cell wall carbohydrates, and this process is performed by the gut microflora, which has evolved to break down every component of plant cell wall (Flint et al., 2008; Martens et al., 2011). Similarly, when intact plant tissue and cells containing drugs reach the gut, commensal microbes gradually digest plant cell walls and release drugs relatively slowly. Furthermore, DT plants biosynthesized both DHAA and artemisinin. DHAA has been shown to have higher bioavailability when compared with pure artemisinin and may play a critical role in the treatment of malaria (Li et al., 1998). However, for clinical translation, this concept should be transferred to proven edible plants for oral delivery studies (Kwon and Daniell, 2016).

Several other biopharmaceuticals have been made in tobacco leaves for the treatment of infectious diseases such as tuberculosis (Lakshmi et al., 2013), cholera (Davoodi-Semiromi et al., 2010), anthrax (Watson et al., 2004; Koya et al., 2005), and plague (Arlen et al., 2008). These could only be tested under field conditions under USDA-APHIS approval (Arlen et al., 2007). Chloroplast engineering is not regulated by USDA-APHIS because this approach does not use plant pathogens or pathogen regulatory sequences (Chan and Daniell, 2015; Kwon and Daniell, 2015). Therefore, DT lines, as created in our study, may have significant regulatory advantages for further development.

In conclusion, we have achieved biosynthesis of the potent anti-malarial drug, artemisinin, in tobacco plants at enhanced levels (~0.8 mg/g dry weight) by introducing two mega-biosynthetic pathways separately into the chloroplast and nuclear genomes, without perturbing the plant health. This is the first report of sequential chloroplast and nuclear genome transformation successfully expressing two mega-biosynthetic pathways and accomplishing complete artemisinin biosynthesis in an alternative host plant.

Most importantly, we report the stability of biosynthesized artemisinin bioencapsulated in plant cells upon oral delivery. The functionality of tobacco DT leaf artemisinin (fed as crushed leaves) was demonstrated by *in vitro* and *in vivo* antimalarial efficacy studies and was considerably better than pure artemisinin. This could significantly increase drug effectiveness and lower the cost of malaria treatment. Malaria disproportionately affects low socio-economic areas and children, the most susceptible to this disease, die in their millions every year. A similar approach could be extended to edible crops, such as lettuce, for artemisinin biosynthesis, and delivering the drug orally may provide a low-cost, environmentally friendly, and supplementary source of bioencapsulated artemisinin, eliminating expensive extraction and purification processes.

## METHODS

### Construction of Plant Transformation Vectors

The tobacco-specific chloroplast transformation vector (pCT-MEV) was designed as reported by Kumar et al. (2012). The nuclear transformation vector pCox-Nuc-Art was designed *in silico*, and contains the genes IDI (IPP/DMAPP isomerase; gi|4633512), FPP synthase (gi|216582) from *E. coli*, a modified amorpha-4,11-diene synthase gene (Anthony et al., 2009), amorpha-4,11-diene C-12 oxidase (*CYP71AV1*, gi|82548247), the *A. annua* cytochrome P450 reductase (*AACPR*, gi|83854016), and the double bond reductase-2 (*DBR2*; gi|494114616). Supplemental Figure 5 contains the entire sequence of vector pCox-Nuc-Art. For efficient expression, each gene was placed under the control of an individual promoter. The APX constitutive promoter (Park et al., 2010) drives the expression of IDI. *CYP71AV1* and *DBR2* were controlled by double enhancer CaMV 35S promoter (Guilley et al., 1982) while FPP and *AACPR* were driven by the CsVMV promoter. The *hpt II* gene, conferring resistance to hygromycin, was placed under the control of CaMV 35S promoter. The DHAA transgene cassette was released from the pUC57 plasmid by double digestion and ligated into the binary vector pCAMBIA1300 (kindly provided by Dr. Narendra Tuteja, ICGEB, New Delhi). Positive clones, confirmed by restriction digestion using enzymes *Bam*HI and *Hin*dIII (NEB, USA), were electroporated into *Agrobacterium* strain EHA105 for nuclear transformation of the T-MEV plants. Transformants were selected on Luria–Bertani plates containing 50 mg/l kanamycin and 10 mg/l rifampicin. In addition, the ADS gene was targeted to mitochondria by use of cox4 mitochondrial signal peptide. AACPR and CYP71AV1 genes were targeted to chloroplasts using a chloroplast transit peptide (gi|20023|emb|X02353.1| Tobacco gene for ribulose 1,5-bisphosphate carboxylase small subunit) and the DBR2 gene was targeted to chloroplasts by the rbcS1 transit peptide.

### Transformation and Selection of Tissues

Chloroplast transformation was performed in *Nicotiana tabacum* cv. Petit Havana SR1 leaves with pCT-MEV vector using S550d gold particles according to manufacturer's instructions (Seashell Technology, CA, USA). Transgenic tissues were selected on RMOP medium containing spectinomycin (500 mg/l). Homoplasmy in the transformed plants (T-MEV) was obtained on antibiotic-containing selection medium. For nuclear transformation, homoplastomic tobacco plants (containing the yeast mevalonate pathway) were re-transformed with *Agrobacterium tumefaciens* (strain EHA105) containing a pCox-Nuc-Art vector. The doubly transformed tissues were selected on RMOP medium containing 50 mg/l hygromycin and 500 mg/l spectinomycin.

### Molecular Analysis of Double Transformants

To test integration of the DHAA biosynthetic cassette, we tested doubly transformed tobacco plants for transgene integration by PCR using gene-specific primers. Primers for *ADS* and *DBR2* are listed in Supplemental Table 1 and were synthesized according to their gene sequence (Sigma, Bengaluru, India).

### Southern Blot Analysis of Double Transformants

Prior to nuclear transformation, homoplasmy of the engineered MEV pathway in the T-MEV plants was confirmed by Southern blot. A hybridization fragment, corresponding to 5.5 kb in the T-MEV plants, confirmed the homoplastomic status of transgenic plants (Supplemental Figure 1B). The hybridization fragment, corresponding to 1.4 kb, represented the native chloroplast genome of wild-type control plants (Supplemental Figure 1B). Transgene copy number in greenhouse-grown, DT plants carrying the pCox-Nuc-Art vector was determined using Southern blots following the DHAA and artemisinin biosynthesis study. Genomic DNA (~15 μg), was isolated from transgenic plants DT1–DT4 and control wild-type plants using a modified CTAB method (Porebski et al., 1997). It was digested overnight with *Eco*RV and separated on a 0.8% agarose gel. It was further transferred to Hybond $N^+$ membranes (GE Healthcare, Buckinghamshire, UK). A PCR-amplified *DBR2* gene (441 bp) was used as a probe (Figure 2A). Probe labeling of DNA blots was carried out using the AlkPhos direct-labeling kit, and signals were detected with the CDP-Star detection reagent (GE Healthcare).

### RNA Transcript Analysis

Total RNA was isolated from wild-type and DT1–DT4 plants using the RNeasy Plant Mini Kit (Qiagen) according to the vendor's instructions. Total RNA was treated with DNase (Qiagen) to remove any remaining genomic DNA contamination. The cDNA synthesis from RNA was carried using the SuperScript III First-strand cDNA synthesis kit (Invitrogen, Carlsbad, CA, USA). The resulting cDNA was amplified using gene-specific primers (Supplemental Table 1) to examine the mRNA transcripts of the transgenes introduced into the nuclear genome of DT plants.

### Analysis of Artemisinin and Intermediate Metabolites

Artemisinin and DHAA levels in leaves of greenhouse-grown DT plants were determined by LC–MS/MS (Suberu et al., 2013), using an Agilent 1200 series reverse-phase C-18 column (4.6 × 100 mm × 3.5 μm) at a flow rate of 0.8 ml/min coupled with a 3200 Q TRAP linear ion trap mass spectrometer (Applied Biosystems, ABSCIEX, Singapore), equipped with a TurboIon spray source. Data were acquired and evaluated by Analyst software (version 1.6, ABSCIEX, Singapore). The MS was operated in positive mode and in MRM (Multiple Reaction Monitoring) mode. Declustering potential (DP), collision energy (CE), and collision cell exit potential (CXP) of each transition were optimized. The major MS/MS fragmentation patterns of both artemisinin (Supplemental Figure 2A) and DHAA were determined. For optimization of MS-dependent parameters, artemisinin (Sigma, Bengaluru, India) and DHAA (Apin Chemicals, Oxon, UK) standards in acetonitrile were injected separately using a gas-tight syringe (Harvard Apparatus, Holliston, USA). Quantification was done using MultiQuant software (Colangelo et al., 2013) and the $R^2$ value was 0.9987.

### Analysis of IPP and DMAPP

Wild-type and DT leaves were lyophilized. Approximately 1 g of each sample was crushed in liquid nitrogen and extracted on ice, for 30 min in methanol (5 ml) in a water bath sonicator (Branson Ultrasonic, Danbury, USA). An IPP (Sigma, Bengaluru, India) standard was diluted with methanol to optimize MS-dependent parameters. The MS was operated in negative ion and MRM mode. Pure IPP was infused at a flow rate of 10 μl/min by a gas-tight syringe (Harvard Apparatus, Holliston, USA). The major MS/MS fragment for IPP (Supplemental Figure 3A), DP, CE, and CXP for each transition were optimized. MRM mode was used to quantify IPP in each sample using MultiQuant software (Colangelo et al., 2013). Metabolites were separated using an Agilent 1200 series reverse-phase C-18 column (4.6 × 100 mm × 3.5 μm) at a flow rate of 0.8 ml/min.

### GC–MS Analysis of Amorphadiene

Leaves from the greenhouse-grown wild-type and DT plants (μ1 g) were crushed in liquid nitrogen and extracted with ethyl acetate (2 ml) for 30 min in a water bath sonicator (Branson Ultrasonic, Danbury, USA). The extracts were concentrated by evaporation under nitrogen. A 1-μl aliquot from the extract was analyzed by GC–MS, using an Agilent 7890A with an HP-5 column (30 m × 0.25 mm internal diameter, 0.25 μm film thickness) and a 7000C triple quadrupole GC–MS/MS spectrometer. The MS was operated in electron ionization mode and scanning mode (50–500 *m*/*z*). Amorphadiene was detected by comparing the retention time and mass spectra with an authentic standard (kindly provided by Amyris Biotechnology, Emeryville, CA, USA).

### *In Vitro* Functionality of Artemisinin against *P. falciparum*

Malarial parasite *in vitro* assays were conducted to test the functionality of DT tobacco-produced artemisinin. A *Plasmodium falciparum* 3D7 culture was synchronized to the ring stage by two consecutive sorbitol treatments separated by 4 h, then cultured for 40 h and allowed to re-invade RBCs and cultured in RPMI-1640 medium (Gibco BRL, Grand Island, USA). Growth inhibition of the *P. falciparum* 3D7 cultures was determined by the SYBR

Green assay (Smilkstein et al., 2004). In brief, a parasite culture with an initial parasitemia of 1%, in 2% hematocrit, was treated with different doses of DT tobacco artemisinin in 96 well plates, each well containing 100 µl of culture of parasite-infected RBCs. DMSO and commercially sourced artemisinin (Sigma-Aldrich, Bengaluru, India) served as negative and positive controls, respectively. Plates containing DT plant extracts and parasites were incubated at 37°C for 48 h. Parasite growth progression was monitored by preparing Giemsa-stained blood smears after 24 h and 48 h. After each time point, 100 µl of lysis buffer (20 mM Tris, 5 mM EDTA, 0.008% saponin, 0.08% Triton X) containing 1×SYBR Green, was added to the cultures and incubated at 37°C for 1 h. Fluorescence was read using a PerkinElmer Victor X3 Multilabel Plate Reader (PerkinElmer, Waltham, MA, USA) at 485/530 nm. The obtained values were plotted, and the $IC_{50}$ of artemisinin was calculated using linear regression analysis.

### *In Vivo* Functionality of Artemisinin in the Murine Model

Cryopreserved blood from *Plasmodium*-infected mice was revived by re-injecting 200 µl of blood intraperitoneally into Balb/C mice. Giemsa-stained blood smears were made to determine percentages of parasitemia. After 1 week a mouse was euthanized, and blood was collected for subsequent experimentation. Four-week-old Balb/C mice were injected with $10^5$ RBCs infected with *P. berghei* and percentage of parasitemia was determined from Giemsa-stained blood smears prepared from the tail region. Mice infected with *P. berghei* were divided into three groups (four mice in each group). One group of mice was orally given a single dose (24 mg/kg) of pure artemisinin drug (Sigma-Aldrich, Bengaluru, India), dissolved in 60 µl of DMSO and reconstituted in water, for nine consecutive days from the third day post infection; the second group of mice was fed oven-dried leaves from DT4 (500 mg), crushed into fine powder with a homogenizer, mixed with 1 ml of water, and fed by gavage needle (18 gauge, curved, 2 inches, and 2.25 mm ball diameter); the third group was fed dried leaves from wild-type plants, prepared as were the DT leaves. All preparations were freshly prepared before the feeding assay and all treatments were performed in parallel. Treated parasite cultures were also analyzed microscopically.

### Statistical Analysis

The differences of artemisinin and IPP produced in wild-type, T-MEV, and doubly transgenic lines (DT1–DT4) were tested by one-way ANOVA with Duncan's multiple range test, followed by a post hoc analysis (Tallarida and Murray, 1987). Analysis of all samples was done in triplicate (n = 3).

## Supplementary Material

Refer to Web version on PubMed Central for supplementary material.

## Acknowledgments

We would like to thank Dr. Chris Paddon of Amyris Biotechnology for providing the amorphadiene standard; Prof. Jay Keasling, UC Berkeley for providing the genes related to biosynthetic pathways, Mr. Girish HR for helping in GC–MS analysis, ICGEB, New Delhi. No conflict of interest declared.

**FUNDING**

This work was supported by the Department of Biotechnology (DBT, grant BT/PR13028/PID/06/473/2009) and Department of Science and Technology (grant SR/SO/BB-37/2010) to S.K., and NIH grants R01 HL 109442, and R01 HL 107904 to H.D.

## References

Anthony JR, Anthony LC, Nowroozi F, Kwon G, Newman JD, Keasling JD. Optimization of the mevalonate-based isoprenoid biosynthetic pathway in *Escherichia coli* for production of the anti-malarial drug precursor amorpha-4, 11-diene. Metab Eng. 2009; 11:13–19. [PubMed: 18775787]

Arlen PA, Falconer R, Cherukumilli S, Cole A, Cole AM, Oishi KK, Daniell H. Field production and functional evaluation of chloroplast-derived interferon-α2b. Plant Biotechnol J. 2007; 5:511–525. [PubMed: 17490449]

Arlen PA, Singleton M, Adamovicz JJ, Ding Y, Davoodi-Semiromi A, Daniell H. Effective plague vaccination via oral delivery of plant cells expressing F1-V antigens in chloroplasts. Infect Immun. 2008; 76:3640–3650. [PubMed: 18505806]

Baldi A, Dixit V. Yield enhancement strategies for artemisinin production by suspension cultures of *Artemisia annua*. Bioresour Technol. 2008; 99:4609–4614. [PubMed: 17804216]

Beale MH, Birkett MA, Bruce TJ, Chamberlain K, Field LM, Huttly AK, Martin JL, Parker R, Phillips AL, Pickett JA. Aphid alarm pheromone produced by transgenic plants affects aphid and parasitoid behavior. Proc Natl Acad Sci USA. 2006; 103:10509–10513. [PubMed: 16798877]

Bertea C, Freije J, Van der Woude H, Verstappen F, Perk L, Marquez V, De Kraker JW, Posthumus M, Jansen B, De Groot A. Identification of intermediates and enzymes involved in the early steps of artemisinin biosynthesis in *Artemisia annua*. Planta Med. 2005; 71:40–47. [PubMed: 15678372]

Bick JA, Lange BM. Metabolic cross talk between cytosolic and plastidial pathways of isoprenoid biosynthesis: unidirectional transport of intermediates across the chloroplast envelope membrane. Arch Biochem Biophys. 2003; 415:146–154. [PubMed: 12831836]

Bogorad L. Engineering chloroplasts: an alternative site for foreign genes, proteins, reactions and products. Trends Biotechnol. 2000; 18:257–263. [PubMed: 10802561]

Brisibe, EA., Chukwurah, PN. Artemisia annua—Pharmacology and Biotechnology. Berlin, Heidelberg: Springer; 2014. Production of artemisinin in planta and in microbial systems need not be mutually exclusive; p. 269-292.

Brown GD, Sy LK. In vivo transformations of dihydroartemisinic acid in *Artemisia annua* plants. Tetrahedron. 2004; 60:1139–1159.

Chan HT, Daniell H. Plant-made oral vaccines against human infectious diseases—are we there yet? Plant Biotechnol J. 2015; 13:1056–1070. [PubMed: 26387509]

Colangelo CM, Chung L, Bruce C, Cheung KH. Review of software tools for design and analysis of large scale MRM proteomic datasets. Methods. 2013; 61:287–298. [PubMed: 23702368]

Covello PS. Making artemisinin. Phytochemistry. 2008; 69:2881–2885. [PubMed: 18977499]

Dalrymple, DG. American Journal of Agricultural Economics. Washington, DC: 2013. *Artemisia annua*, Artemisinin, ACTs and Malaria Control in Africa: Tradition, Science and Public Policy.

Davies MJ, Atkinson CJ, Burns C, Woolley JG, Hipps NA, Arroo RR, Dungey N, Robinson T, Brown P, Flockart I. Enhancement of artemisinin concentration and yield in response to optimization of nitrogen and potassium supply to Artemisia annua. Ann Bot. 2009; 104:315–323. [PubMed: 19483202]

Davies M, Atkinson C, Burns C, Arroo R, Woolley J. Increases in leaf artemisinin concentration in *Artemisia annua* in response to the application of phosphorus and boron. Ind Crops Prod. 2011; 34:1465–1473.

Davoodi-Semiromi A, Schreiber M, Nalapalli S, Verma D, Singh ND, Banks RK, Chakrabarti D, Daniell H. Chloroplast-derived vaccine antigens confer dual immunity against cholera and malaria by oral or injectable delivery. Plant Biotechnol J. 2010; 8:223–242. [PubMed: 20051036]

Dudareva N, Andersson S, Orlova I, Gatto N, Reichelt M, Rhodes D, Boland W, Gershenzon J. The nonmevalonate pathway supports both monoterpene and sesquiterpene formation in snapdragon flowers. Proc Natl Acad Sci USA. 2005; 102:933–938. [PubMed: 15630092]

Efferth T. Molecular pharmacology and pharmacogenomics of artemisinin and its derivatives in cancer cells. Curr Drug Targets. 2006; 7:407–421. [PubMed: 16611029]

Efferth T, Herrmann F, Tahrani A, Wink M. Cytotoxic activity of secondary metabolites derived from *Artemisia annua* L. towards cancer cells in comparison to its designated active constituent artemisinin. Phytomedicine. 2011; 18:959–969. [PubMed: 21831619]

Elfawal MA, Towler MJ, Reich NG, Weathers PJ, Rich SM. Dried whole-plant *Artemisia annua* slows evolution of malaria drug resistance and overcomes resistance to artemisinin. Proc Natl Acad Sci USA. 2015; 112:821–826. [PubMed: 25561559]

Enserink M. Source of new hope against malaria is in short supply. Science. 2005; 307:33. [PubMed: 15637249]

Farhi M, Marhevka E, Ben-Ari J, Algamas-Dimantov A, Liang Z, Zeevi V, Edelbaum O, Spitzer-Rimon B, Abeliovich H, Schwartz B. Generation of the potent anti-malarial drug artemisinin in tobacco. Nat Biotechnol. 2011a; 29:1072–1074. [PubMed: 22158354]

Farhi M, Marhevka E, Masci T, Marcos E, Eyal Y, Ovadis M, Abeliovich H, Vainstein A. Harnessing yeast subcellular compartments for the production of plant terpenoids. Metab Eng. 2011b; 13:474–481. [PubMed: 21601648]

Ferreira J, Simon J, Janick J. Relationship of artemisinin content of tissue-cultured, greenhouse-grown, and field-grown plants of *Artemisia annua*. Planta Med. 1995; 61:351–355. [PubMed: 17238088]

Flint HJ, Bayer EA, Rincon MT, Lamed R, White BA. Polysaccharide utilization by gut bacteria: potential for new insights from genomic analysis. Nat Rev Microbiol. 2008; 6:121–131. [PubMed: 18180751]

Fuentes P, Zhou F, Erban A, Karcher D, Kopka J, Bock R. A new synthetic biology approach allows transfer of an entire metabolic pathway from a medicinal plant to a biomass crop. Elife. 2016; 5:e13664. [PubMed: 27296645]

Gao S, Shen S, Wang G, Niu J, Lin A, Pan G. PSI-driven cyclic electron flow allows intertidal macro-algae *Ulva* sp (Chlorophyta) to survive in desiccated conditions. Plant Cell Physiol. 2011; 52:885–893. [PubMed: 21471121]

Goldstein JL, Brown MS. Regulation of the mevalonate pathway. Nature. 1990; 343:425–430. [PubMed: 1967820]

Graham IA, Besser K, Blumer S, Branigan CA, Czechowski T, Elias L, Guterman I, Harvey D, Isaac PG, Khan AM. The genetic map of *Artemisia annua* L. identifies loci affecting yield of the antimalarial drug artemisinin. Science. 2010; 327:328–331. [PubMed: 20075252]

Gry M, Rimini R, Strömberg S, Asplund A, Pontén F, Uhlén M, Nilsson P. Correlations between RNA and protein expression profiles in 23 human cell lines. BMC Genomics. 2009; 10:365. [PubMed: 19660143]

Guilley H, Dudley RK, Jonard G, Balàzs E, Richards KE. Transcription of cauliflower mosaic virus DNA: detection of promoter sequences, and characterization of transcripts. Cell. 1982; 30:763–773. [PubMed: 7139714]

Ikram NKB, Zhan X, Pan XW, King BC, Simonsen HT. Stable heterologous expression of biologically active terpenoids in green plant cells. Front Plant Sci. 2015; 6:129. [PubMed: 25852702]

Kappers IF, Aharoni A, Van Herpen TW, Luckerhoff LL, Dicke M, Bouwmeester HJ. Genetic engineering of terpenoid metabolism attracts bodyguards to *Arabidopsis*. Science. 2005; 309:2070–2072. [PubMed: 16179482]

Khanuja SPS, Paul S, Shasany AK, Gupta AK, Darokar MP, Gupta MM, Verma RK, Ram G, Kumar A, Lal RK. High Artemisinin Yielding *Artemisia* Plant Named 'CIM-Arogya': U.S. Patent. 2008; 7:375, 260.

Kindermans JM, Pilloy J, Olliaro P, Gomes M. Ensuring sustained ACT production and reliable artemisinin supply. Malar J. 2007; 6:125. [PubMed: 17868471]

Kohli N, Westerveld DR, Ayache AC, Verma A, Shil P, Prasad T, Zhu P, Chan SL, Li Q, Daniell H. Oral delivery of bioencapsulated proteins across blood–brain and blood–retinal barriers. Mol Ther. 2014; 22:535–546. [PubMed: 24281246]

Koya V, Moayeri M, Leppla SH, Daniell H. Plant-based vaccine: mice immunized with chloroplast-derived anthrax protective antigen survive anthrax lethal toxin challenge. Infect Immun. 2005; 73:8266–8274. [PubMed: 16299323]

Koyama T, Katsuki Y, Ogura K. Studies on isopentenyl pyrophosphate isomerase with artificial substrates: ZE isomerization of Z-3-methyl-3-pentenyl pyrophosphate. Bioorg Chem. 1983; 12:58–70.

Kumar S, Hahn FM, Baidoo E, Kahlon TS, Wood DF, McMahan CM, Cornish K, Keasling JD, Daniell H, Whalen MC. Remodeling the isoprenoid pathway in tobacco by expressing the cytoplasmic mevalonate pathway in chloroplasts. Metab Eng. 2012; 14:19–28. [PubMed: 22123257]

Kwon KC, Daniell H. Low-cost oral delivery of protein drugs bioencapsulated in plant cells. Plant Biotechnol J. 2015; 13:1017–1022. [PubMed: 26333301]

Kwon KC, Daniell H. Oral delivery of protein drugs bioencapsulated in plant cells. Mol Ther. 2016; 24:1342–1350. [PubMed: 27378236]

Kwon KC, Nityanandam R, New JS, Daniell H. Oral delivery of bioencapsulated exendin-4 expressed in chloroplasts lowers blood glucose level in mice and stimulates insulin secretion in beta-TC6 cells. Plant Biotechnol J. 2013; 11:77–86. [PubMed: 23078126]

Lakshmi PS, Verma D, Yang X, Lloyd B, Daniell H. Low cost tuberculosis vaccine antigens in capsules: expression in chloroplasts, bio-encapsulation, stability and functional evaluation in vitro. PLoS One. 2013; 8:e54708. [PubMed: 23355891]

Li Z, Sharkey TD. Metabolic profiling of the methylerythritol phosphate pathway reveals the source of post-illumination isoprene burst from leaves. Plant Cell Environ. 2013; 36:429–437. [PubMed: 22831282]

Li QG, Peggins JO, Fleckenstein LL, Masonic K, Heiffer MH, Brewer TG. The pharmacokinetics and bioavailability of dihydroartemisinin, arteether, artemether, artesunic acid and artelinic acid in rats. J Pharm Pharmacol. 1998; 50:173–182. [PubMed: 9530985]

Limaye A, Koya V, Samsam M, Daniell H. Receptor-mediated oral delivery of a bioencapsulated green fluorescent protein expressed in transgenic chloroplasts into the mouse circulatory system. FASEB J. 2006; 20:959–961. [PubMed: 16603603]

Lützow M, Beyer P. The isopentenyl-diphosphate Δ-isomerase and its relation to the phytoene synthase complex in daffodil chromoplasts. Biochim Biophys Acta. 1988; 959:118–126.

Martens EC, Lowe EC, Chiang H, Pudlo NA, Wu M, McNulty NP, Wade Abbott D, Henrissat B, Gilbert HJ, Bolam DN. Recognition and degradation of plant cell wall polysaccharides by two human gut symbionts. PLoS Biol. 2011; 9:2492.

Martin VJ, Pitera DJ, Withers ST, Newman JD, Keasling JD. Engineering a mevalonate pathway in *Escherichia coli* for production of terpenoids. Nat Biotechnol. 2003; 21:796–802. [PubMed: 12778056]

Olsson ME, Olofsson LM, Lindahl AL, Lundgren A, Brodelius M, Brodelius PE. Localization of enzymes of artemisinin biosynthesis to the apical cells of glandular secretory trichomes of *Artemisia annua* L. Phytochemistry. 2009; 70:1123–1128. [PubMed: 19664791]

Paddon C, Westfall P, Pitera D, Benjamin K, Fisher K, McPhee D, Leavell M, Tai A, Main A, Eng D. High-level semi-synthetic production of the potent antimalarial artemisinin. Nature. 2013; 496:528–532. [PubMed: 23575629]

Page JE, Hause G, Raschke M, Gao W, Schmidt J, Zenk MH, Kutchan TM. Functional analysis of the final steps of the 1-deoxy-D-xylulose 5-phosphate (DXP) pathway to isoprenoids in plants using virus-induced gene silencing. Plant Physiol. 2004; 134:1401–1413. [PubMed: 15064370]

Park SH, Yi N, Kim YS, Jeong MH, Bang SW, Do Choi Y, Kim JK. Analysis of five novel putative constitutive gene promoters in transgenic rice plants. J Exp Bot. 2010; 61:2459–2467. [PubMed: 20363869]

Pasoreck EK, Su J, Silverman IM, Gosai SJ, Gregory BD, Yuan JS, Daniell H. Terpene metabolic engineering via nuclear or chloroplast genomes profoundly and globally impacts off-target pathways through metabolite signalling. Plant Biotechnol J. 2016; 14:1862–1875. [PubMed: 27507797]

Porebski S, Bailey LG, Baum BR. Modification of a CTAB DNA extraction protocol for plants containing high polysaccharide and polyphenol components. Plant Mol Biol Rep. 1997; 15:8–15.

Saxena B, Subramaniyan M, Malhotra K, Bhavesh NS, Potlakayala SD, Kumar S. Metabolic engineering of chloroplasts for artemisinic acid biosynthesis and impact on plant growth. J Biosci. 2014; 39:33–41. [PubMed: 24499788]

Shapira MY, Resnick IB, Chou S, Neumann AU, Lurain NS, Stamminger T, Caplan O, Saleh N, Efferth T, Marschall M. Artesunate as a potent antiviral agent in a patient with late drug-resistant cytomegalovirus infection after hematopoietic stem cell transplantation. Clin Infect Dis. 2008; 46:1455–1457. [PubMed: 18419454]

Sherman A, Su J, Lin S, Wang X, Herzog RW, Daniell H. Suppression of inhibitor formation against factor VIII in hemophilia A mice by oral delivery of antigens bioencapsulated in plant cells. Blood. 2014; 124:1659–1668. [PubMed: 24825864]

Shil PK, Kwon KC, Zhu P, Verma A, Daniell H, Li Q. Oral delivery of ACE2/Ang-(1-7) bioencapsulated in plant cells protects against experimental uveitis and autoimmune uveoretinitis. Mol Ther. 2014; 22:2069–2082. [PubMed: 25228068]

Smilkstein M, Sriwilaijaroen N, Kelly JX, Wilairat P, Riscoe M. Simple and inexpensive fluorescence-based technique for high-throughput antimalarial drug screening. Antimicrob Agents Chemother. 2004; 48:1803–1806. [PubMed: 15105138]

Smith TC, Weathers PJ, Cheetham RD. Effects of gibberellic acid on hairy root cultures of *Artemisia annua*: growth and artemisinin production. In Vitro Cell Dev Biol Plant. 1997; 3:75–79.

Suberu J, Song L, Slade S, Sullivan N, Barker G, Lapkin AA. A rapid method for the determination of artemisinin and its biosynthetic precursors in *Artemisia annua* L. crude extracts. J Pharm Biomed Anal. 2013; 84:269–277. [PubMed: 23867088]

Svensson US, Ashton M. Identification of the human cytochrome P450 enzymes involved in the in vitro metabolism of artemisinin. Br J Clin Pharmacol. 1999; 48:528–535. [PubMed: 10583023]

Tallarida, RJ., Murray, RB. Manual of Pharmacologic Calculations with Computer Programs. New York: Springer-Verlag; 1987.

Ting HM, Wang B, Rydén AM, Woittiez L, Herpen T, Verstappen FW, Ruyter-Spira C, Beekwilder J, Bouwmeester HJ, Krol A. The metabolite chemotype of *Nicotiana benthamiana* transiently expressing artemisinin biosynthetic pathway genes is a function of CYP71AV1 type and relative gene dosage. New Phytol. 2013; 199:352–366. [PubMed: 23638869]

Utzinger J, Xiao SH, Tanner M, Keiser J. Artemisinins for schistosomiasis and beyond. Curr Opin Investig Drugs. 2007; 8:105–116.

van Herpen TW, Cankar K, Nogueira M, Bosch D, Bouwmeester HJ, Beekwilder J. *Nicotiana benthamiana* as a production platform for artemisinin precursors. PLoS One. 2010; 5:e14222. [PubMed: 21151979]

Vogel C, Marcotte EM. Insights into the regulation of protein abundance from proteomic and transcriptomic analyses. Nat Rev Genet. 2012; 13:227–232. [PubMed: 22411467]

Wallaart TE, Bouwmeester HJ, Hille J, Poppinga L, Maijers NCA. Amorpha-4,11-diene synthase: cloning and functional expression of a key enzyme in the biosynthetic pathway of the novel antimalarial drug artemisinin. Planta. 2001; 212:460–465. [PubMed: 11289612]

Watson J, Koya V, Leppla SH, Daniell H. Expression of *Bacillus anthracis* protective antigen in transgenic chloroplasts of tobacco, a non-food/feed crop. Vaccine. 2004; 22:4374–4384. [PubMed: 15474731]

Weathers PJ, Elfawal MA, Towler MJ, Acquaah-Mensah GK, Rich SM. Pharmacokinetics of artemisinin delivered by oral consumption of *Artemisia annua* dried leaves in healthy vs. *Plasmodium chabaudi*-infected mice. J Ethnopharmacol. 2014; 153:732–736. [PubMed: 24661969]

White NJ. Qinghaosu (artemisinin): the price of success. Science. 2008; 320:330–334. [PubMed: 18420924]

Wu S, Schalk M, Clark A, Miles RB, Coates R, Chappell J. Redirection of cytosolic or plastidic isoprenoid precursors elevates terpene production in plants. Nat Biotechnol. 2006; 24:1441–1447. [PubMed: 17057703]

Yang K, Monafared RS, Wang H, Lundgren A, Brodelius PE. The activity of the artemisinic aldehyde Δ11 (13) reductase promoter is important for artemisinin yield in different chemotypes of *Artemisia annua*. L Plant Mol Biol. 2015; 88:325–340. [PubMed: 25616735]

Zhang Y, Teoh KH, Reed DW, Maes L, Goossens A, Olson DJ, Ross AR, Covello PS. The molecular cloning of artemisinic aldehyde Δ11(13) reductase and its role in glandular trichome-dependent

biosynthesis of artemisinin in *Artemisia annua*. J Biol Chem. 2008; 283:21501–21508. [PubMed: 18495659]

Zhang Y, Nowak G, Reed DW, Covello PS. The production of artemisinin precursors in tobacco. Plant Biotechnol J. 2011; 9:445–454. [PubMed: 20723135]

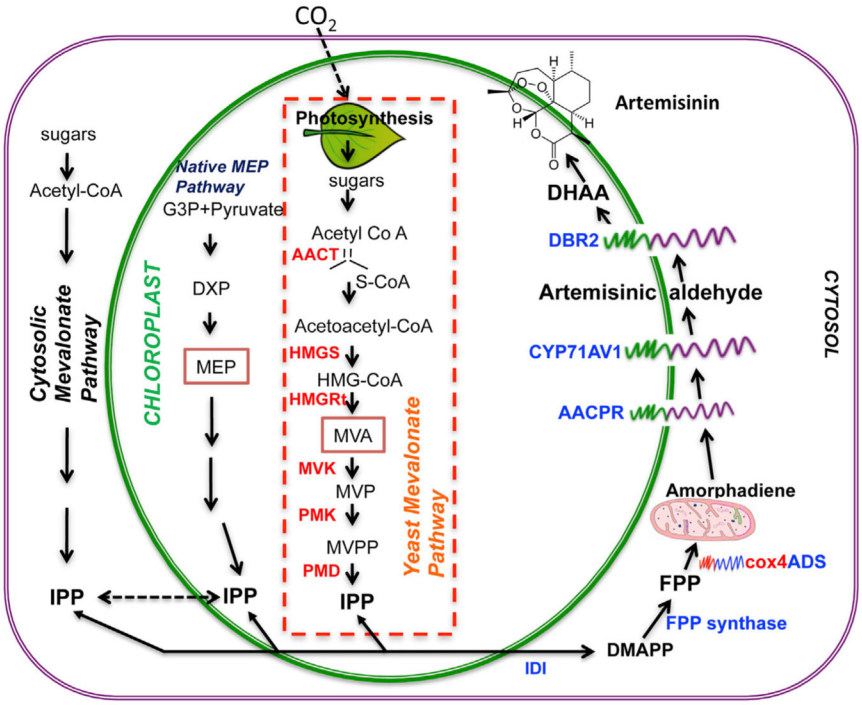


**Figure 1. Schematic Representation of Artemisinin Biosynthesis by Sequential Metabolic Engineering of Chloroplast and Nuclear Genomes**

Six genes, AACT, HMGS, HMGRt, MVK, PMK, and PMD (in red font and inside a dotted rectangle, Supplemental Figure 1A) encoding yeast MEV pathway were integrated into the chloroplast genome using a biolistic approach to generate an elevated IPP pool. Six genes (*ADS*, *CYP71AV1*, *AACPR*, *DBR2*, IDI, and FPP) of the artemisinin biosynthetic pathway were integrated into the nuclear genome of homoplastomic plants (Supplemental Figure 1B) using vector pNuc-cox-ART. Subcellular targeting of DBR2, AACPR, and CYP71AV1 were mediated by a chloroplast transit peptide (Figure 2A). Dihydroartemisinic acid (DHAA) converts itself to artemisinin via photochemical oxidation, a non-enzymatic reaction. AACT, acetoacetyl CoA thiolase; HMGS, HMGCoA synthase; HMGRt, C-terminal truncated HMGCoA reductase; MVK, mevalonate kinase; PMK, phosphomevalonate kinase; PMD, mevalonate pyrophosphate decarboxylase; DXP, 1-Deoxy-D-xylulose 5-phosphate; MEP, 2-C-methyl-D-erythritol 4-phosphate; IPP, isopentenyl diphosphate; IDI, IPP isomerase; DMAPP, dimethylallyl pyrophosphate; ADS, amorphadiene synthase; FPP, farnesyl diphosphate; CYP71AV1, amorpha-4,11-diene C-12 oxidase; AACPR, *Artemisia annua* cytochrome P450 reductase; DBR2, double bond reductase2.

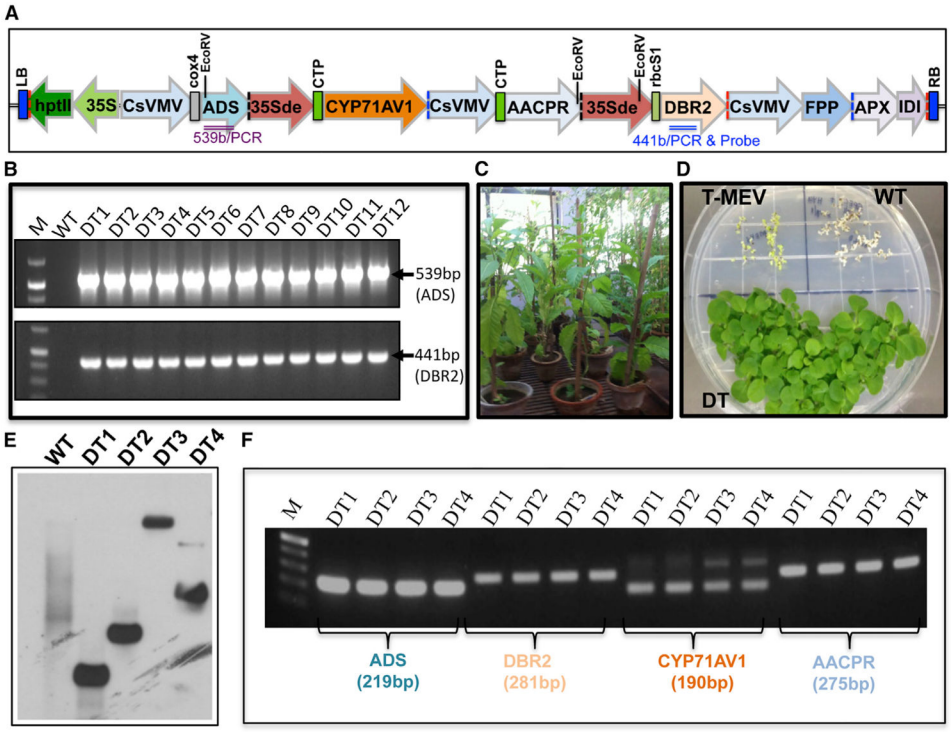


**Figure 2. Nuclear Genome Transformation of Homoplastomic Plant**

(**A**) Physical map of the DHAA biosynthetic pathway vector pNuc-cox-Art.

(**B**) PCR products amplified using primers ADS-F and ADS-R (marked by purple in **A**) and DBR2-F and DBR2-R (marked by blue in **A**) from 12 doubly transgenic (DT1–DT12) plants yielded a 539-bp and 441-bp amplicon, respectively. No PCR products were observed in wild-type (WT) plants.

(**C**) DT plants transferred to a greenhouse grew normally like WT plants and set seeds.

(**D**) Seeds of matured DT plants germinated and seedlings grew well on double-selection medium containing hygromycin (50 mg/l) and spectinomycin (500 mg/l). T-MEV and WT plants lacking essential transgenes conferring resistance to both antibiotics could not germinate on double-selection medium (see also Supplemental Figure 1).

(**E**) Four transgenic lines namely DT1–DT4, with elevated artemisinin and DHAA contents were examined for copy number. Genomic DNA (~15 μg) from DT1–DT4 and WT plants digested with *Eco*RV were analyzed by Southern blot using *DBR2* as probe (shown as blue line in vector **A**).

(**F**) Total RNA was isolated from DT1–DT4 and resulting cDNAs were amplified using gene-specific RT–PCR primers of *ADS*, *DBR2*, *AACPR*, and *CYP71AV1*.

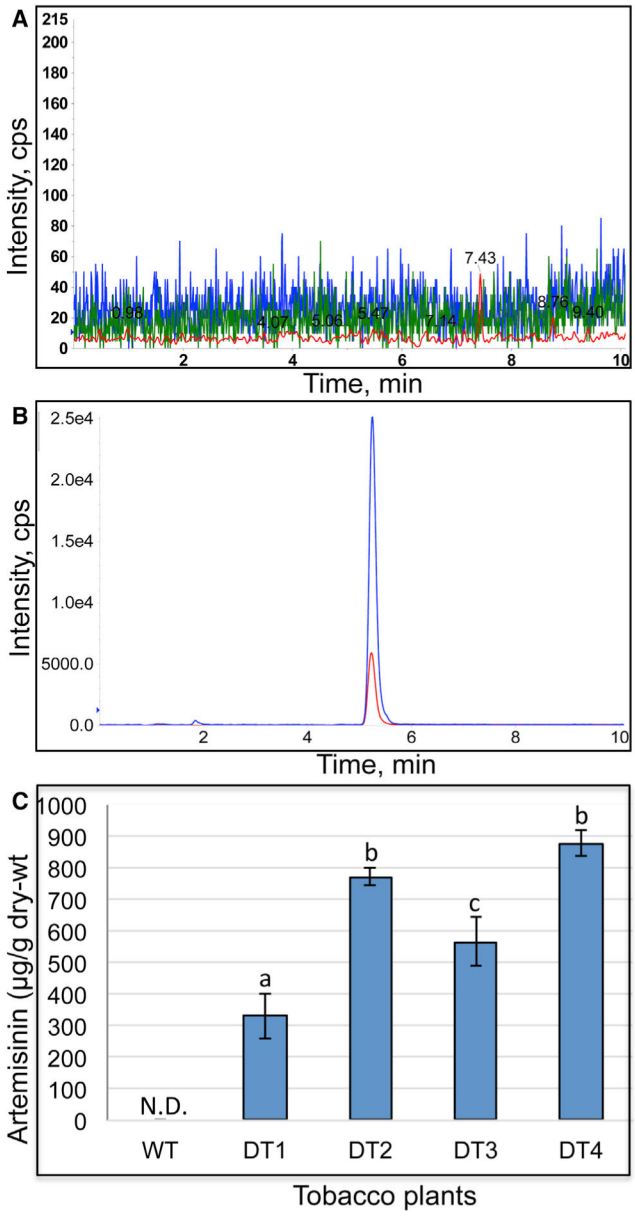


**Figure 3. LC–MS/MS Analysis of Artemisinin Biosynthesized in Double-Transformed Plants**

(**A**) Chromatographic profile of wild-type plant extract, analyzed in MRM mode for artemisinin detection.

(**B**) Extracted ion chromatogram for artemisinin–MRM transition (*m*/*z* 283–209) standard peak shown in red. The artemisinin peak of transgenic (DT4) shown in blue is overlaid with standard peak (red) at ~5.25 min. No such corresponding peak for artemisinin was observed in extracts of wild-type (**A**).

(**C**) Artemisinin yield quantified in DTs by MultiQuant (ABSciex, Singapore) (see also Supplemental Table 3). Standard curve was plotted and the $R^2$ coefficient was 0.998. ANOVA followed by Duncan's multiple range test demonstrated that the mean artemisinin levels were significantly different among the lines ($P < 0.01$). Means followed by the same

alphabets are not significantly different by Duncan's multiple range test at $P < 0.01$, $n = 3$. Data are represented as mean ± SD. N.D., not determined; WT, wild-type.

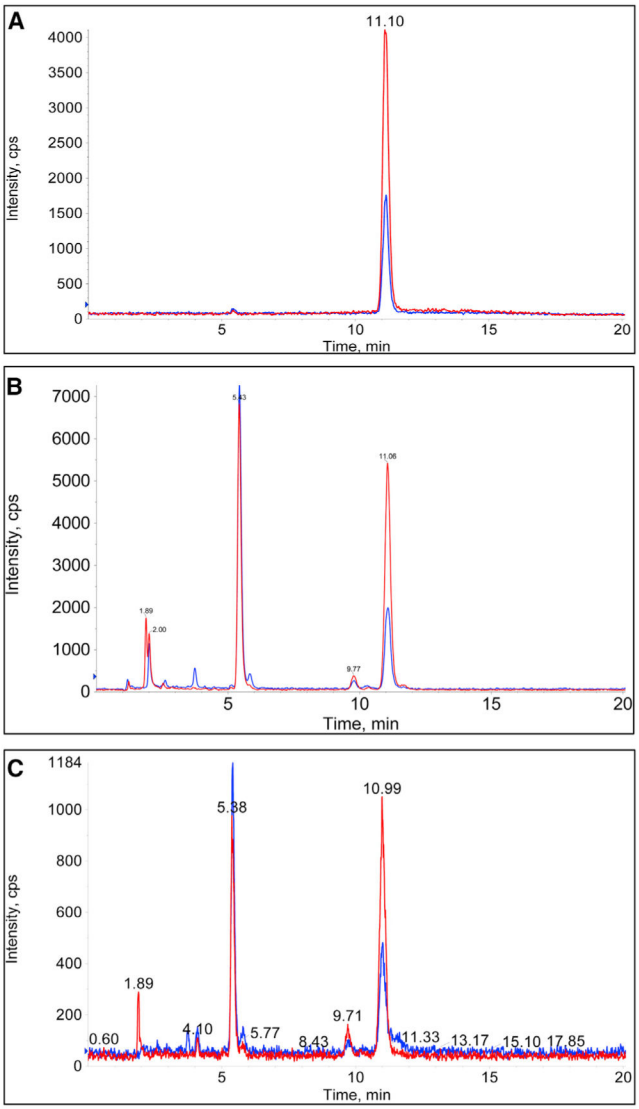


**Figure 4. LC–MS/MS Analysis of Dihydroartemisinic Acid Biosynthesized in DT Plants**

(**A–C**) Extracted ion chromatogram for dihydroartemisinic acid (DHAA)–MRM transitions for two fragments *m*/*z* 237–163 and *m*/*z* 237–107. (**A**) Standard DHAA peak at retention time ~11 min. (**B**) DHAA in DT4. (**C**) Similar peak was observed in *Artemisia annua* extract. An unknown peak was seen at retention time 5.25 min in both DT4 and *A. annua* samples. The red and blue lines denote the MRM transitions (163 and 107) for the parent ion *m*/*z* 237 DHAA.

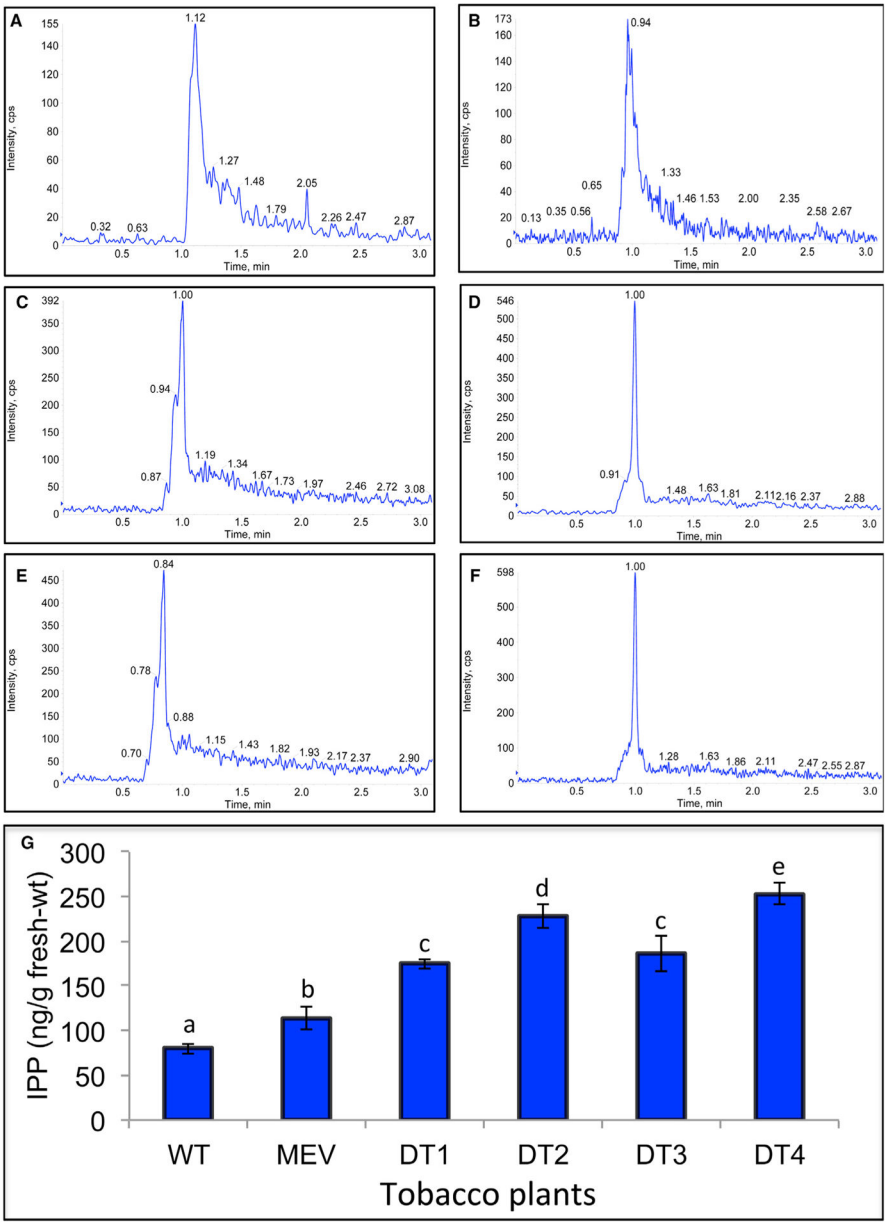


**Figure 5. Comparative LC–MS/MS Analysis of Intermediate Isoprenoid IPP-Metabolite Levels in Controls (Wild-Type) and Chloroplast Transgenic with Mevalonate Pathway (MEV) and Double-Transformed Plants (DT1–DT4)**

(**A–G**) Extracted ion chromatogram of MRM transition (*m*/*z* 245–159) for IPP (see also Supplemental Figure 3) in (**A**) wild-type, (**B**) MEV, and (**C–F**) DT1–DT4. (**G**) IPP yield quantified in wild-type (WT), MEV, and DTs by MultiQuant (ABSciex, Singapore). A standard curve was plotted and the $R^2$ coefficient was 0.998. Analysis of variance (ANOVA) followed by Duncan's multiple range test demonstrated that the mean IPP levels were significantly different among the lines ($P < 0.01$). Means followed by the same alphabets are not significantly different by Duncan's multiple range test at $P < 0.01$, n = 3. Data are represented as mean ± SD.

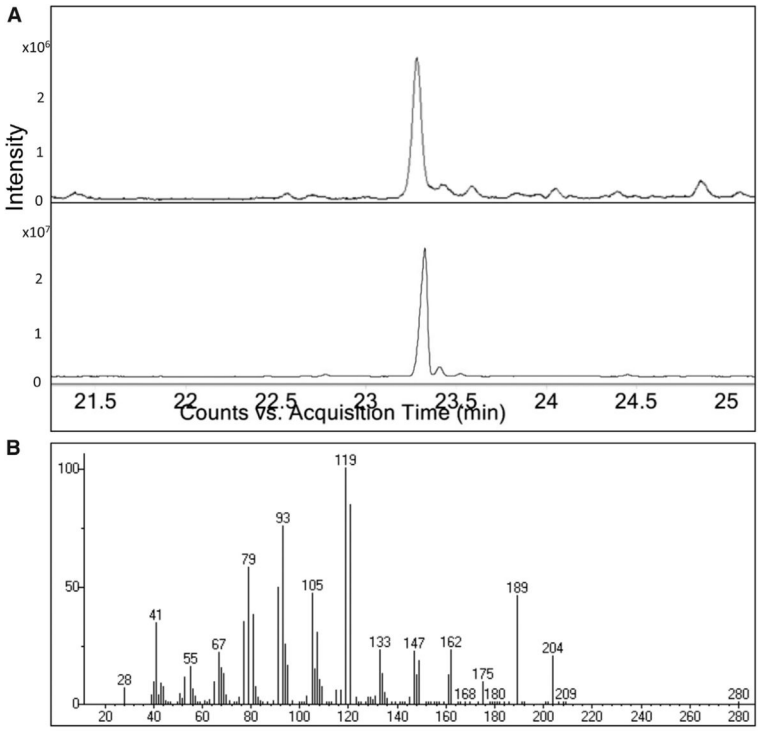


**Figure 6. Accumulation of Amorphadiene in DT4**

(**A**) Total ion chromatograms from ethyl acetate extract of DT4 plant (upper) and amorphadiene standard (lower). Peak corresponding to amorphadiene was observed at retention time ~23 min in the chromatogram of DT4 and amorphadiene standard.

(**B**) Mass spectra of amorphadiene obtained from the peak in DT4 plant at retention time ~23 min in GC profile.

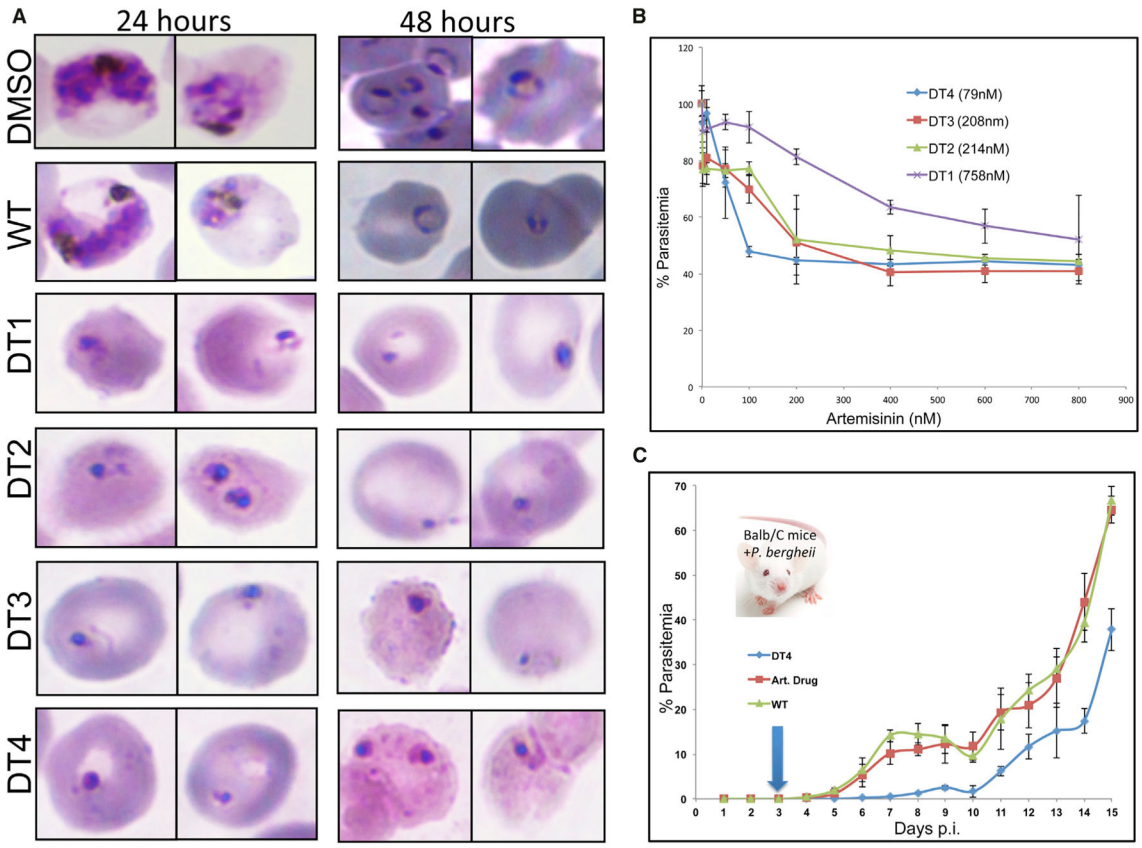


**Figure 7. *In Vitro* and *In Vivo* Efficacy of Artemisinin Biosynthesized in Dual Metabolically Engineered Plants**

(**A**) *In vitro* mortality assay of artemisinin from double transformed (DTs) on RBCs infected with *Plasmodium falciparum* 3D7. Giemsa staining of RBCs infected with *P. falciparum 3D7*. No mortality on parasite growth was seen in DMSO, wild-type (WT), and schizonts at the end of 48 h matured to release the ring-stage parasites. DT1–DT4 extracts controlled parasite growth in 24–48 h assay.

(**B**) $IC_{50}$ values were plotted and calculated using linear regression analysis (see also Supplemental Figure 4).

(**C**) Balb/C mice infected with *Plasmodium berghei* were orally fed for nine consecutive days (3–11) with dried DT4 leaves (dose equivalent to 24 mg/kg), control wild-type (WT), and pure drug (Art. drug; equivalent to 24 mg/kg). Arrow in the graph represents the start of oral feeding on the third day post infection. The error bars represent mean parasitemia ± SD.

**Table 1**

Metabolite Profile in Tobacco Lines (DT1–DT4) Engineered with DHAA Biosynthetic Pathway.

| Metabolites | WT | T-MEV | DT1 | DT2 | DT3 | DT4 |
|---|---|---|---|---|---|---|
| Artemisinin | ND | ND | 331 ± 71 | 773 ± 27 | 567 ± 76 | 877 ± 40 |
| Dihydroartemisinic acid | ND | ND | 62 ± 3 | 91 ± 6 | 82 ± 3 | 150 ± 10 |
| Amorphadiene | ND | ND | 10 ± 5 | 53 ± 8 | 32 ± 5 | 60 ± 5 |
| IPP/DMAPP | 80 ± 6 | 114 ± 12 | 175 ± 13 | 228 ± 5 | 186 ± 13 | 253 ± 20 |
| Squalene | 2.77 ± 0.1 | 10 ± 0.5 | 27 ± 0.5 | 22 ± 1.1 | 26 ± 0.4 | 21 ± 0.1 |

Values are mean ± SD. ND, not detected. Yield of all metabolites is mentioned in μg/g dry weight except for IPP/DMAPP, which is expressed as ng/g fresh weight, and squalene as μg/g fresh weight. All values have been rounded to the nearest integer.